Fabrication of magnetic tunnel junctions with a metastable bcc Co$_3$Mn disordered alloy as a bottom electrode

Kazuma Kunimatsu[1,2], Tomoki Tsuchiya[3,4][*], Kelvin Elphick[5] Tomohiro Ichinose[2],

Kazuya Z. Suzuki[2,4], Atsufumi. Hirohata[5], Shigemi Mizukami[2,3,4][†],

[1]*Department of Applied Physics, Graduate School of Engineering, Tohoku University, Sendai 980-8579,*

Japan [2]*WPI Advanced Institute for Materials Research, Tohoku University, Katahira 2-1-1, Sendai*

980-8577, Japan [3]*Center for Science and Innovation in Spintronics (CSIS), Core Research Cluster (CRC),*

Tohoku University, Sendai 980-8577, Japan [4]*Center for Spintronics Research Network (CSRN), Tohoku*

University, Sendai 980-8577, Japan [5]*Department of Electronic Engineering, The University of York, York*

YO10 5DD, England

We fabricated MgO barrier magnetic tunnel junctions (MTJs) with a Co$_3$Mn alloy bottom and FeCoB top electrodes. The (001)-oriented epitaxial films of the metastable bcc Co$_3$Mn disordered alloys obtained showed saturation magnetization of approximately 1640 emu/cm^3. The transmission electron microscopy showed that the MgO barrier was epitaxially grown on the Co$_3$Mn electrode. Tunnel magnetoresistance of approximately 150% was observed at room temperature after the annealing of MTJs at 350°C, indicating that bcc Co$_3$Mn alloys have relatively high spin polarization.

The magnetic tunnel junction (MTJ) is a key device for spintronics,[1–3] which has been utilized in various magnetic sensors including the read head of a hard disk drive, magnetoresistive random access memory, and neuromorphic applications.[4–6] One of the issues is to enhance the tunnel magnetoresistance (TMR) effect, i.e., junction resistance change depending on the parallel and antiparallel states of two magnetizations for the junctions. Currently, the MgO barrier and FeCoB alloy electrodes are used as the standard MTJ barrier and magnetic materials,[7–11] which exhibited the record 604% in the TMR ratio at room temperature (RT).[12] Such a high TMR ratio is attributed to the orbital symmetry filtering by the MgO barrier and the highly spin polarized Δ_1 band in FeCo alloys.[13,14] To search for routes to further enhance the TMR ratio, it is curious to investigate various magnetic metals other than FeCo binary systems.

Here, we report the TMR effect observed in MTJs utilizing different types of dis-

[*]E-mail: tomoki.tsuchiya.d1@tohoku.ac.jp

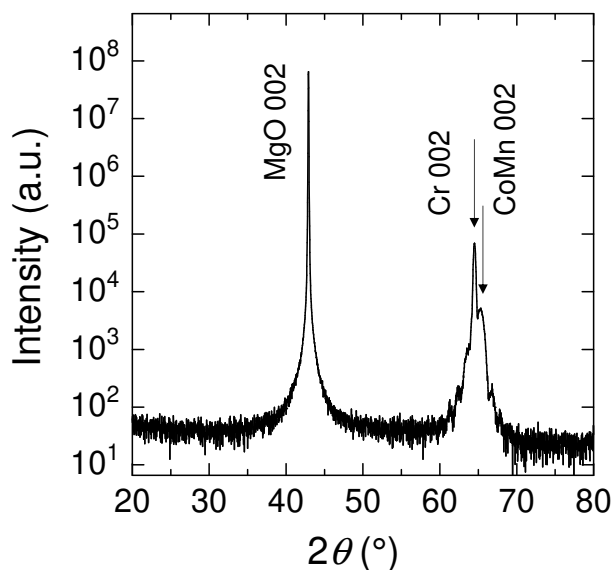[†]E-mail: shigemi.mizukami.a7@tohoku.ac.jp

Fig. 1. Out-of-plane XRD pattern for Co$_3$Mn film deposited on (001) Cr-buffered MgO substrate.

1 ordered bcc CoMn alloy. A bulk Co-rich CoMn binary disordered alloy has a hcp or

2 fcc phase as thermodynamically stable phase.[15–18] The saturation magnetizations and

3 Curie temperatures decrease with increasing Mn concentration, and a magnetic long

4 range order is lost around the Mn concentration of 30–35%.[15–18] In contrast, metastable

5 bcc phase of Co-rich CoMn alloys show the relatively high saturation magnetization at

6 similar Mn composition,[19–21] and a net magnetic moment per atom is in 2.32–2.53 μ_B

7 at Mn concentration of 24%,[21] being close to that of a bcc Fe. This bcc phase is ob-

8 tained in thin films grown on (001) GaAs and (001) MgO single crystalline substrates by

9 molecular beam epitaxy (MBE) technique, as reported by a few groups.[19–21] However,

10 there are no reports on MTJs comprised of bcc CoMn alloy electrodes to date.

11   All samples were deposited on (100) MgO single crystal substrates using a magnetron

12 sputtering technique. The base pressure was 2×10^{-7} Pa. The MTJ staking structure was

13 substrate/ Cr(40)/ Co$_3$Mn(10)/ Mg(0.4)/ MgO(2)/ Fe$_{60}$Co$_{20}$B$_{20}$(4.5)/ Ta(3)/ Ru(5)

14 (thickness in nm). All layers were deposited at RT. The composition of Co$_3$Mn film

15 is Co$_{74}$Mn$_{26}$ (at.%) determined using inductively-coupled plasma mass spectrometer.

16 We also prepared samples of substrate/ Cr(40)/ Co$_3$Mn(10)/ Mg(0.4)/ MgO(2)/ Ta(2)

17 for structural and magnetization measurements. The crystal structures of the samples

18 were determined using an x-ray diffractometer (XRD) by Cu K_α radiation. Nanostruc-

19 tural analysis of samples was conducted by transmission electron microscopy (TEM).

20 Magnetization measurements were performed using a vibrating sample magnetometer.
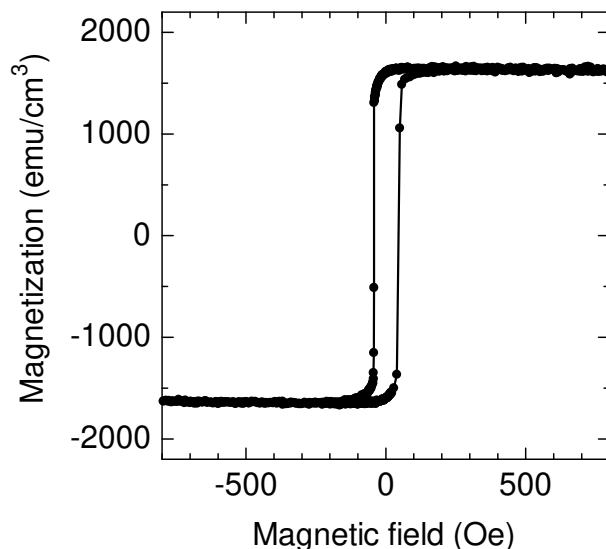
Fig. 2. In-plane magnetization hysteresis loop for the Co_3Mn film deposited on (001) Cr buffered MgO substrate.

1 The microfabrication of the MTJs were performed using a standard ultraviolet photo-
2 lithography and Ar ion milling. The thirty six junctions with rectangular shapes were
3 obtained on the substrate with the junction areas of 60×15, 40×10, 20×5, 40×2, 15×3,
4 and 20×2 μm^2. The MTJs were annealed with a vacuum furnace at the temperature
5 range 250–400°C. Magnetoresistance (MR) for the MTJs was measured by a four-probe
6 method using a prober system with a maximum applied field of approximately 1 kOe.
7 All the measurements were performed at RT.

8   Out-of-plane XRD pattern of the Co_3Mn film is shown in Fig. 1. The 002 peaks from
9 the Cr buffer layer and bcc Co_3Mn were observed, but no other peaks, in particular
10 those from fcc Co-Mn, were detected. The out-of-plane lattice parameter for the Co_3Mn
11 film was evaluated as approximately 0.286 nm, which is close to the lattice constant
12 for the bcc Co_3Mn of 0.285 nm.[19] Thus, it is considered that the (001)-oriented bcc
13 Co_3Mn films were obtained on (001) Cr-buffered MgO substrates.

14   The in-plane magnetization curve is shown in Fig. 2. The saturation magnetization
15 M_s is approximately 1640 emu/cm³. This value is comparable to that of Co or Fe
16 and is also similar to the magnetic moment value evaluated by x-ray magnetic circular
17 dichroism for bcc $Co_{76}Mn_{24}$ alloy films,[21] rather than that of fcc CoMn alloys with the
18 similar Mn concentration.[16]

19   The MR curves measured at RT for the 40×2 μm^2. MTJ annealed at 350°C is shown
20 in Fig. 3(a). The resistance changes depending on the magnetization configuration are
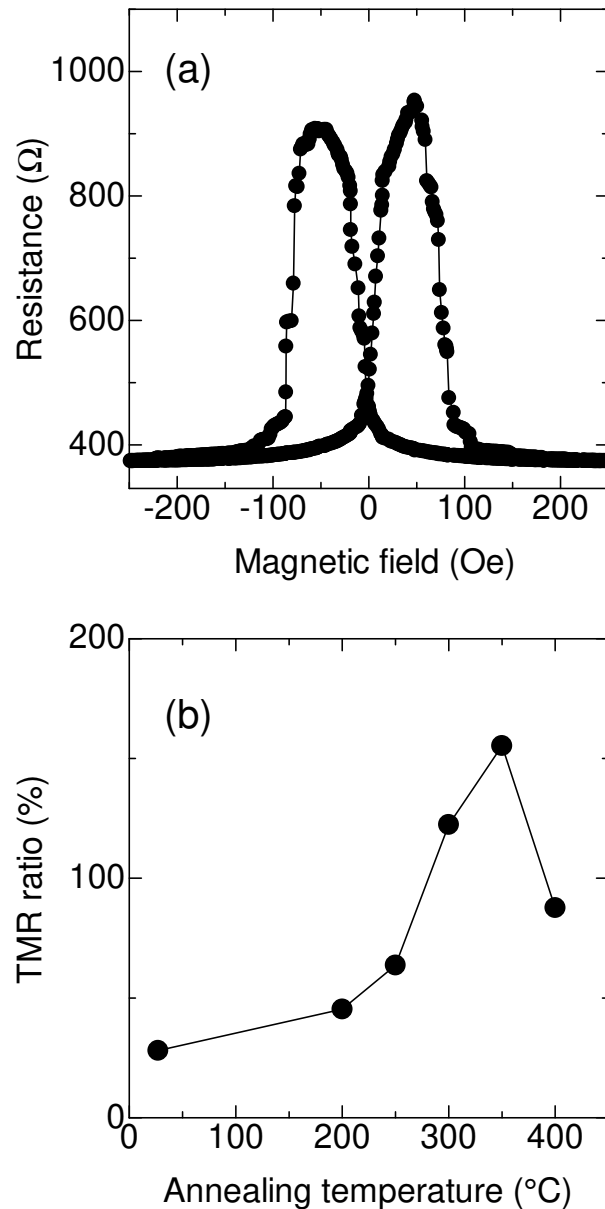
Fig. 3. (a) The typical MR curve for MTJs with Co₃Mn film as the bottom electrode. (b) The TMR ratio as a function of the annealing temperature of the MTJ with Co₃Mn film as the bottom electrode.

observed. Note that the MTJ is a pseudo-spin valve type, which means that both magnetic layers were unpinned by the exchange bias[12] and the antiparallel state would not be well defined in this study. Figure 3(b) shows the TMR ratio for this junction as a function of the annealing temperature of the MTJ. The maximum TMR ratio was observed as 155% at the annealing temperature of 350°C in Fig. 3(b) and was 158% for the different MTJ on the same substrate. This value is smaller than the TMR ratio of ∼200% observed at RT in Fe/MgO/Fe fully-epitaxial MTJs fabricated by the MBE

1 technique.[22]

2   Figure 4 shows the cross sectional TEM image for the MTJ sample annealed at
3 350°C. The MgO barrier is epitaxially grown on the bcc (001) Co_3Mn electrode. More-
4 over, the coherency of the lattices of Co_3Mn, MgO, and almost crystallized FeCoB at
5 the bottom and top interfaces are visible. These observations mean that the coherent
6 tunneling is expected if the bcc Co_3Mn has the Δ_1 band at the Fermi level.

7   To gain insight into the spin polarization of the bcc Co_3Mn studied here, Julliere's
8 model was used for approximate estimation, which can be expressed as[1]

$$\text{TMR ratio } (\%) = \frac{2P_1P_2}{1 - P_1P_2} \times 100, \tag{1}$$

9 where P_1 and P_2 are the tunneling spin polarization for each magnetic electrode. Since
10 this relation is hold only for an incoherent tunneling, the evaluate spin polarization
11 should be regarded as an effective value in case of the coherent tunneling. To account
12 for the TMR ratio observed in this study using this relation, the tunneling spin polar-
13 ization for bcc Co_3Mn with MgO barrier should be at least 0.44 at RT if the tunneling
14 spin polarization of FeCoB is 1 . This is relatively higher than the spin polarization
15 of 0.33 evaluated at low temperature in $Co_{73}Mn_{27}$ alloy, which had a low saturation
16 magnetization and was unlikely bcc phase.[23] A more detailed discussion is beyond the
17 scope of this brief report and will be provided elsewhere.

18   In summary, we fabricated Co_3Mn/MgO/FeCoB MTJs using the sputtering tech-
19 nique. The (001)-oriented metastable bcc Co_3Mn epitaxial films obtained exhibited
20 saturation magnetization of approximately 1640 emu/cm^3. The cross-sectional TEM
21 showed that the MgO barrier was epitaxially grown on the Co_3Mn electrode. We ob-
22 served the TMR ratio of 158% at RT for MTJs annealed at 350°C, indicating that
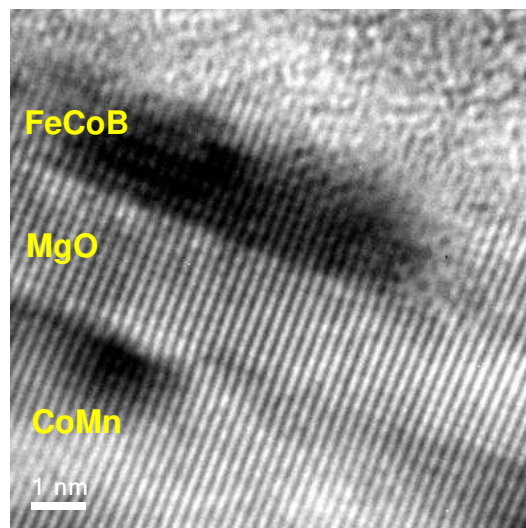23 metastable bcc Co_3Mn alloys have relatively high spin polarization.

Fig. 4.   The cross-sectional TEM image for the MTJ sample.

References

1) M. Julliere, Phys. Lett. A **54,** 225 (1975).

2) T. Miyazaki and N. Tezuka, J. Magn. Magn. Mater. **139,** L231 (1995).

3) J.S. Moodera, L.R. Kinder, T.M. Wong, and R. Meservey, Phys. Rev. Lett. **74,** 3273 (1995).

4) J.-G. (Jimmy) Zhu and C. Park, Mater. Today **9,** 36 (2006).

5) A.D. Kent and D.C. Worledge, Nat. Nanotechnol. **10,** 187 (2015).

6) M. Romera, P. Talatchian, S. Tsunegi, F. Abreu Araujo, V. Cros, P. Bortolotti, J. Trastoy, K. Yakushiji, A. Fukushima, H. Kubota, S. Yuasa, M. Ernoult, D. Vodenicarevic, T. Hirtzlin, N. Locatelli, D. Querlioz, and J. Grollier, Nature **563,** 230 (2018).

7) S. Yuasa, T. Nagahama, A. Fukushima, Y. Suzuki, and K. Ando, Nat. Mater. **3,** 868 (2004).

8) S.S.P. Parkin, C. Kaiser, A. Panchula, P.M. Rice, B. Hughes, M. Samant, and S.-H. Yang, Nat. Mater. **3,** 862 (2004).

9) S. Yuasa, T. Katayama, T. Nagahama, A. Fukushima, H. Kubota, Y. Suzuki, and K. Ando, Appl. Phys. Lett. **87,** 222508 (2005).

10) S. Yuasa, A. Fukushima, H. Kubota, Y. Suzuki, and K. Ando, Appl. Phys. Lett. **89,** 042505 (2006).

11) D.D. Djayaprawira, K. Tsunekawa, M. Nagai, H. Maehara, S. Yamagata, N. Watanabe, S. Yuasa, Y. Suzuki, and K. Ando, Appl. Phys. Lett. **86,** 092502 (2005).

12) S. Ikeda, J. Hayakawa, Y. Ashizawa, Y.M. Lee, K. Miura, H. Hasegawa, M. Tsunoda, F. Matsukura, and H. Ohno, Appl. Phys. Lett. **93,** 082508 (2008).

13) J. Mathon and A. Umerski, Phys. Rev. B **63,** 220403 (2001).

14) W.H. Butler, X.-G. Zhang, T.C. Schulthess, and J.M. MacLaren, Phys. Rev. B **63,** 054416 (2001).

15) J.S. Kouvel, J. Phys. Chem. Solids **16,** 107 (1960).

16) M. Matsui, T. Ido, K. Sato, and K. Adachi, J. Phys. Soc. Japan **28,** 791 (1970).

17) A. Z. Menshikov, G. A. Takzei, Yu. A. Dorofeev, V. A. Kazan- stev, A. K. Kostyshin, and I. I. Sych, Zh. Eksp. Teor. Fiz. **89,** 1269 (1985) [Sov. Phys. JETP **62,** 734 (1985)].

18) K. Ishida and T. Nishizawa, Bull. Alloy Phase Diagrams **11,** 125 (1990).

1 19) D. Wu, G.L. Liu, C. Jing, Y.Z. Wu, D. Loison, G.S. Dong, X.F. Jin, and D.-S.

2   Wang, Phys. Rev. B **63,** 214403 (2001).

3 20) L. Zhang, D. Basiaga, J.R. O'Brien, and D. Heiman, J. Appl. Phys. **98,** 106101

4   (2005).

5 21) R.J. Snow, H. Bhatkar, A.T. N'Diaye, E. Arenholz, and Y.U. Idzerda, J. Magn.

6   Magn. Mater. **419,** 490 (2016).

7 22) F. Bonell, T. Hauet, S. Andrieu, F. Bertran, P. Le Févre, L. Calmels, A. Tejeda,

8   F. Montaigne, B. Warot-Fonrose, B. Belhadji, A. Nicolaou, and A.

9   Taleb-Ibrahimi, Phys. Rev. Lett. **108,** 176602 (2012).

10 23) T.H. Kim and J.S. Moodera, Phys. Rev. B **66,** 104436 (2002).